Environ Model Assess (2006) 11:179–194
DOI 10.1007/s10666-006-9044-8

ORIGINAL PAPER

Modeling of oak pollen dispersal on the landscape level with a mesoscale atmospheric model

Silvio Schueler · Katharina Heinke Schlünzen

Received: 6 May 2005 / Accepted: 18 February 2006

Abstract We present the extension and application of the mesoscale atmospheric meteorology model METRAS for dispersion of oak pollen. We incorporated functions for pollen emission, pollen viability and pollen deposition into METRAS and simulated pollen dispersal on a scale of up to 200 km. The basis of the simulations is a real landscape structure that includes topography, land use, and the location and size of oak stands. We simulated the oak pollen dispersion of one single oak stand with an estimated annual pollen production of 1 billion pollen grains/m^2 forest surface on two exemplary days of the flowering season in 2000. Depending on the meteorological situation of the simulated days, a pollen cloud with about 10 pollen/m^3 may extend up to 30 km from the source. Downstream of the oak stand, approximately 1,000 pollen/m^2 deposited up to a distance of 25 km, and lower amounts of pollen deposited up to 100 km away. These values of pollen concentration and deposition lay within the range of published field studies. Overall, it is shown that mesoscale atmospheric models are applicable to simulate pollen dispersal on the landscape level.

Keywords *Quercus robur* · pollen dispersal · pollen emission · pollen production · gene flow · mesoscale model · landscape level

S. Schueler
Institute for Forest Genetics and Forest Tree Breeding,
Federal Research Centre for Forestry and Forest Products,
Sieker Landstr. 2,
D-22927 Grosshansdorf, Germany

S. Schueler (✉)
Department of Genetics, Federal Research
and Training Centre for Forests,
Natural Hazards and Landscape,
Hauptstr. 7, A-1140 Vienna, Austria
e-mail: silvio.schueler@bfw.gv.at

K. H. Schlünzen
Meteorological Institute, Center for Marine and Climate
Research, University of Hamburg,
Bundesstraße 55,
D-20146 Hamburg, Germany

1. Introduction

Pollen dispersal is a crucial process in the life cycle of wind-pollinated trees. It provides reproduction and gene flow, and contributes significantly to the genetic diversity within and among populations [28]. A proper understanding of pollen dispersal is important for the management and conservation of tree species in increasingly fragmented landscapes [36], for the risk assessment of transgenic tree species [9], and for a deeper understanding of adaptive and evolutionary processes in spatial structured populations [3, 11]. Furthermore, the pollen of several tree species act as major allergen in the human population, with increasing prevalence in many parts of the world [1]. This also makes forecasting of pollen dispersal an urgent demand of the health care system.

Pollen dispersal can be estimated by in situ measurements using pollen traps or genetic markers. The first method produces estimates of the 'potential pollen flow' [26], if traps are used around a known pollen source. Such studies give an impression of the strong and wide-ranging pollen dispersal of wind-pollinated trees [25, 38]. For example, 9.5 oak pollen

grains/mm^2 were collected after 3 days of a sampling surface on the Isle of Helgoland, which is situated in the North Sea about 70 km offshore and on which no oak trees were growing [38]. However, pollen traps allow only measurements on a few selected locations, and the results are affected by the location of the trap and do not give an overall estimate on pollen dispersion of one tree or forest. In addition, meteorological factors influence the transport and settling, and thus data from one experiment do not necessarily reflect the pollen dispersion found in another year.

In contrast, quantification of gene flow based on genetic markers permits the estimation of 'effective pollen flow.' The use of genetic fingerprint and paternity analysis with nuclear DNA microsatellites [13] has considerably improved our knowledge on pollen dispersal. In wind-pollinated tree species, various studies have shown a high impact of pollen from outside a small study area [10, 55]. Analysis of the pollen dispersal of *Quercus macrocarpa* in a fragmented landscape showed a mean pollen dispersal of about 75 m within the stand, and a high percentage (~62%) of pollen immigrants from outside the investigated forest [10]. This illustrates the problem arising from direct paternity approaches: the paternity can only be assigned if all potential fathers have been sampled and analyzed. Thus, reliable estimates of pollen dispersal with paternity analysis are only possible on a local scale of a few hundred meters, and the origin of about 60% of pollen cannot be inferred [10, 55]. The 'Two Generation' approach was developed to overcome this problem [54]. Based on genetic data of progenies from single seed mother trees, this approach calculates the mean pollen dispersal indirectly, without knowing every potential father tree.

Modeling of pollen dispersion (i) can overcome the limitations of the experimental approaches, (ii) can help to generalize the observed pattern, and (iii) can be applied for the prediction of pollen concentration and deposition in terms of forest management, risk assessment of transgenic trees, and as a health care service. Recent efforts to predict the potential gene flow of transgenic crops has led to the development and validation of several mechanistical and quasi-mechanistical models for pollen flow [14, 15, 24, 27]. These models deal with pollen dispersal on scales of up to 1 km, but do not consider transport to larger distances and detailed impact of meteorology on pollen emission or dispersion. On the other hand, several models have been developed to forecast the pollen concentration of allergy-inducing species, some of which include pollen emission and dispersion processes on regional scales [16, 18, 19, 22, 23, 33, 53].

In this article, we extend the non-hydrostatic mesoscale model METRAS [39] for oak pollen emission and transport, and use it to study the release, transport and settling of oak pollen during 2 days of the flowering period in the year 2000. Our objectives were to (i) develop a parameterization for the pollen emission of oak, (ii) use empirically determined values of pollen production, and (iii) compare the simulation results with previous studies concerning pollen emission, pollen concentration, and pollen deposition to allow an evaluation of the modeling approach for gene flow studies on the landscape level. The study area is situated in Northern Germany and encloses a fragmented landscape with several oak stands (figure 1).

2. Model description

The atmospheric mesoscale model METRAS is used to simulate the meteorological conditions, and the release, transport, and deposition of oak pollen. METRAS has been successfully applied to study atmospheric phenomena in different regions [8, 29, 30, 42, 52] and with consideration of pollution transport [43, 44, 49, 58, 60].

METRAS is based on the fundamental conservation principles of fluid dynamics, namely, those of mass, momentum and energy. Wind, temperature, humidity, and cloud and rainwater are calculated from prognostic equations, and pressure and density from diagnostic ones. Reynolds averaging and a first-order turbulence closure are applied [29]. The concentration of pollen is calculated on an Eulerian grid by solving the conservation of mass equation in flux form:

$$\underbrace{\frac{\partial \overline{C}_\zeta}{\partial t}}_{(a)} = \underbrace{-\nabla\left(\overline{C}\,\overline{v}\right)}_{(b)} \underbrace{-\nabla\left(\overline{C'v'}\right)}_{(c)} + \underbrace{Q_{emi}}_{(d)} + \underbrace{Q_{sed}}_{(e)} - \underbrace{Q_{viab}}_{(f)}. \quad (1)$$

The temporal change (a) of the average concentration of viable pollen grains results from the advection (b), turbulent diffusion (c), pollen emission (d), pollen sedimentation and settling (e) and from the pollen viability (f). To describe the advection and diffusion processes, the average wind $\overline{v}$ and its turbulent fluctuations $\mathbf{v}'$ need to be known. Average winds are calculated from the momentum equations, thereby fulfilling the anelastic approximation. Turbulent diffusion processes are parameterized with a first-order closure scheme with inclusion of the counter

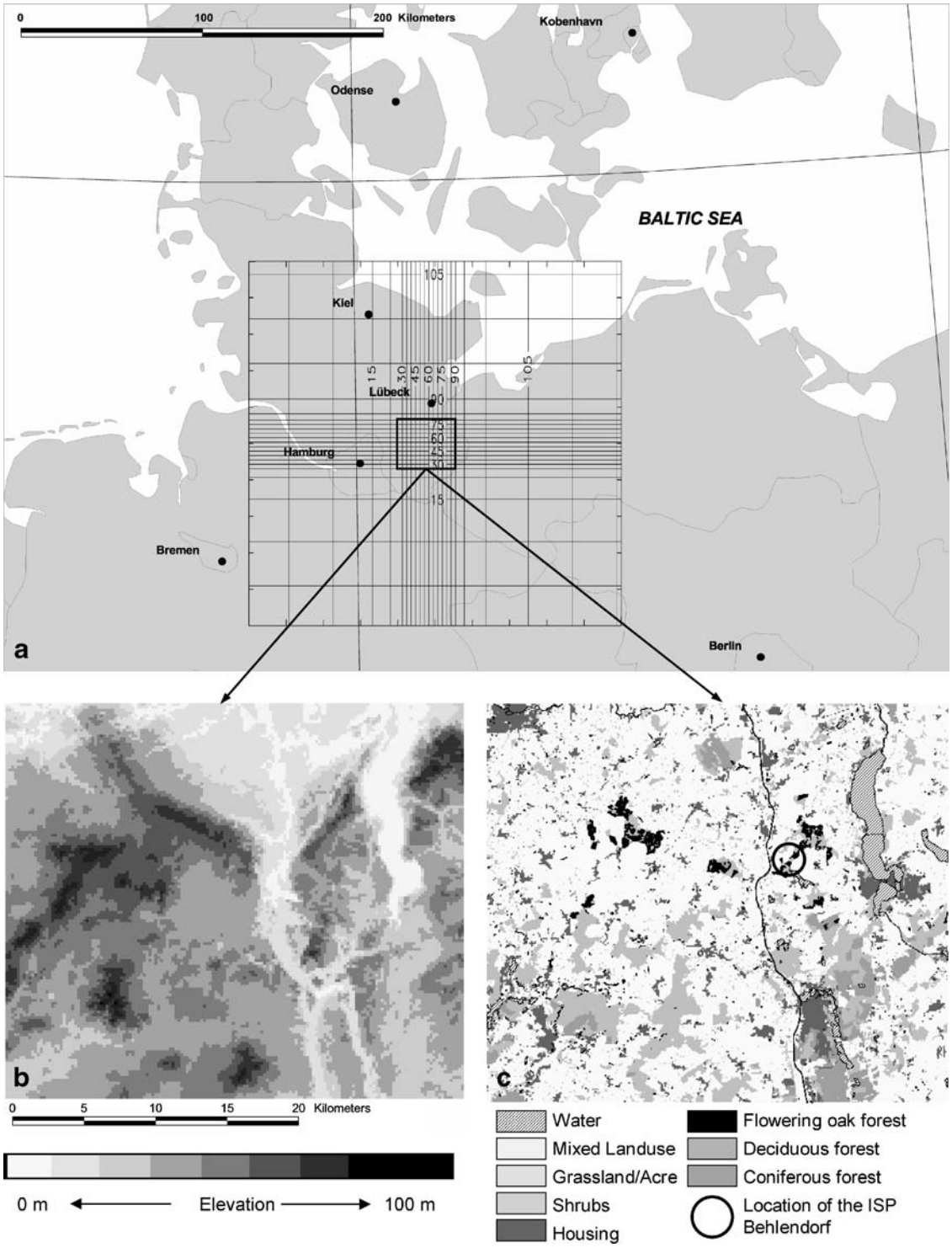

Figure 1 Location and characteristics of the investigated landscape. (a) Location of the simulated region with a schematic representation of the applied horizontal non-uniform grid. The grid size within the marked core region is 500 × 500m and increases up to 5,000 × 5,000m outside of the core area. (b) Topography data of the core region (DGM200). (c) Land-use data of the core region (Basis DLM) with the integrated digital oak map and the location of the intensive study plot (ISP) Behlendorf

gradient term for convective conditions [29]. Sub-grid-scale land uses are considered by application of the blending-height concept that uses a flux averaging approach [59]. The pollen emission (d) and the viability (f) depend on the meteorological factors as described below, whereas the sedimentation and deposition (e) of the pollen is set as a constant settling velocity with respect to pollen size.

Table 1 Nomenclature.

$\underline{APQ}$	Absolute pollen quantities
$\overline{C_\zeta}$	Average pollen concentration
d	Number of days since flowering started
Δt	Model time step
k	Fraction of viable pollen grains on the total number of pollen grains
N	Duration of flowering period [days]
p_R	Pollen production ratio of a given day D
P_A	Actual pollen production
P_{ED}	Estimated potential pollen production of a given day D within the flowering period
P_T	Total pollen production within the flowering period
P_{Ts}	Potential pollen production per second
Q_{emi}	Pollen emission
Q_{sed}	Pollen sedimentation and deposition
Q_{viab}	Pollen reduction due to decrease of viability
r_S	Pollen sensitivity to sunlight [s^{-1}]
RH	Relative humidity
RPQ	Relative pollen quantities
RSW	Short wave radiation [W m^{-2} s^{-1}]
T	Temperature [°C]
$\lvert\nu\rvert$	Measured wind speed
$\overline{\nu}, \nu'$	Average wind velocity and its turbulent fluctuations
VPD	Water vapor pressure deficit
V_S	Pollen survival rate

2.1. Pollen emission

The pollen emission Q_{emi} is a function of the total pollen production P_T during a flowering period of n days, with the actual pollen production P_A dependent on the actual meteorological conditions. The relations used are derived from experimental data.

The pollen release of oak in northern Germany occurs during 4–6 weeks, beginning in the second half of April and continuing up to the end of May [61]. The exact start of the flowering period, the length of the period, and the intensity of flowering vary from year to year. Our simulations, however, do not include the calculation of a whole flowering period. We restrict our simulations to two typical days of the flowering period of year 2000 and use the oak pollen counts in Lübeck to calculate the daily pollen emission. Lübeck is located approximately 20 km north of the oak stand we want to study. Pollen data are recorded at Lübeck on a routine basis by the German Pollen Foundation, using Hirst volumetric traps [20] and standard analysis [61].

The day-to-day variation in oak flowering intensity within the flowering period is described following an idea of Norris-Hill [31], who used a cubic function for grass pollen emission. We found a fourth-order polynomial curve to fit best to the oak pollen counts at Lübeck for year 2000 (figure 2):

$$P_{ED} = \max\begin{pmatrix}-16.633 + 66.267d - 6.5771d^2 \\ + 0.2217d^3 - 0.0025d^4, 0\end{pmatrix}. \quad (2)$$

Equation (2) describes the potential pollen concentration (P_{ED}) as the number of mature oak anthers and dependent on the number of flowering days (d), with d=1 for the first flowering day. Under the assumption that the pollen concentration data from Lübeck are representative of the regional average pollen production, equation (2) can be used to calculate the pollen production ratio (p_R) of a single day dependent on the pollen production of the complete flowering period consisting of N days:

$$p_R = \frac{P_{ED}}{P_T} \text{ with } P_T = \sum_{d=1}^{N} P_{ED}. \quad (3)$$

The pollen release varies during a day dependent on the actual meteorological conditions. This relation was deduced by regression analysis from pollen counts

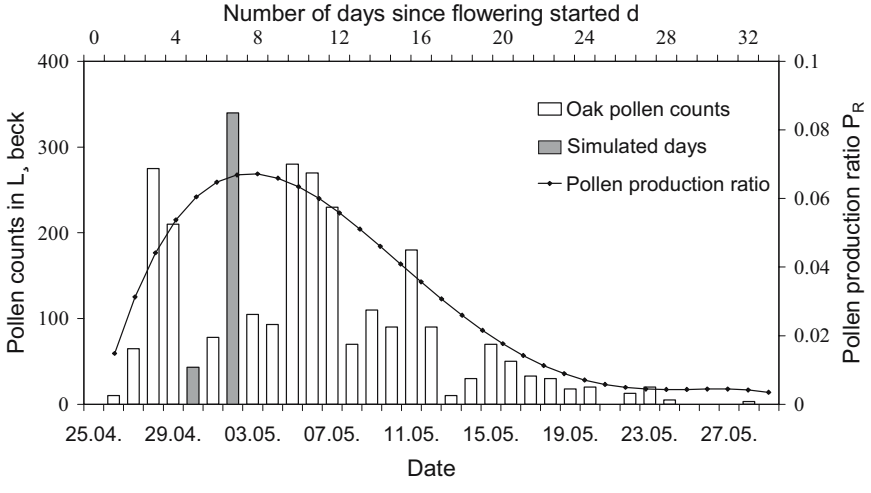

Figure 2 Oak pollen counts in Lübeck during flowering period in 2000. The function for the flowering rate displayed in the figure is given by equation (2)

within an alder crown (*Alnus glutinosa*) and two-hourly measurements of meteorological conditions quantified on two consecutive days [38]. This kind of data set is – to our knowledge – very rare, and Rempe's data set taken in 1937 [38] is the most complete one ever published. It combines measurements of meteorological variables ($|v|$, wind speed; RH, relative humidity; T, temperature) and pollen concentration of a wind pollinated tree in a high temporal resolution. Regression analysis of pollen concentrations on the given meteorological parameters identified that only the dependence of the number of emitted pollen grains from water vapor pressure deficit (VPD) was approximately the same for both days. Thus, the most relevant meteorological parameter is VPD that was calculated from the measured values (Appendix A). Dependence of pollen emission on other meteorological parameters than VPD were neglected, and the following function was used in METRAS:

$$P_A = \begin{cases} \Delta t P_{Ts}(33VPD - 42) \; for \; VPD > 1.273, \\ 0 \; else. \end{cases} \quad (4)$$

The relative number of emitted pollen grains per square meter oak forest (P_A) in each model time step Δt is calculated dependent on the total pollen production of 1 m^2 oak forest, expressed as potential number of pollen grains per second (P_{Ts}), and on VPD. The total pollen production of 1 m^2 oak forest stand was estimated by field observations as described below.

2.2. Pollen production

The total annual pollen production P_T of a forest, a single oak tree or 1 m^2 of oak crown has not been published in the literature up to now. To obtain a rough estimate of the total pollen production, we counted the number of male catkins that were shed after the pollen release in 2003. On April 30, we randomly distributed 20 woody frames on the forest floor of a mixed stand of deciduous trees in which pedunculate oak represented 78% of the main population. Each frame had a size of 1 m^2 and was strung with a rough fly screen. The frames were emptied on May 8, 15, 22 and June 4. The frames were finally emptied and removed on June 18 after all trees had visually shed their catkins and after two strong windstorms on June 8 and 11. The mean number of catkins on 1 m^2 was 1,760. The mean number of oak pollen grains per catkin was estimated to be 555,768 for *Q. petraea* [35]. The mean number of catkins on 1 m^2 oak forest and the mean number of oak pollen grains per catkin resulted in a total annual pollen production (P_T) of 0.978 billion (about 1×10^9) pollen grains produced by 1 m^2 oak forest stand. This value was used as P_T in the simulations.

2.3. Pollen viability

To investigate the biological relevance of pollen dispersal, it is essential to study not only the physical transport, but also the biological effectiveness of the pollen grain as it changes in dependence of the flight conditions and the duration of the transport. Therefore, a contemporaneous study was conducted in which the percentage of viable pollen grains and the decrease of the pollen viability with increasing duration of solar radiation were assessed [48]. This study determined (i) the fraction of viable pollen grains k on the total number of pollen, and (ii) the exponential decrease of viability with continuing irradiation. The second term is introduced with the equation:

$$V_S = e^{\left(\frac{-r_S \Delta t R_{SW}}{250\left(Wm^{-2}\right)}\right)}, \quad (5)$$

where the pollen survival rate V_S is expressed as an exponential function of pollen sensitivity to sunlight (r_S in s^{-1}), the model time step (Δt), and the incoming short wave radiation (R_{SW} in Wm^{-2}). The fraction of viable pollen grains k was determined as 0.59, and the pollen sensitivity to sunlight r_S was $4.567 \times 10^5 s^{-1}$ as average value of three oak trees within two consecutive years [48]. V_S is computed every model time step using the actual short wave radiation at every grid point. The pollen concentration received after integrating equation (1) is multiplied by V_S in order to consider the viability. A general consideration of the loss of viability in Eulerian models is given in Appendix B.

2.4. Pollen sedimentation and deposition

Settling of the pollen depends on pollen size. For small pollen, the influence of plant surfaces needs to be considered, which is also relevant for gas exchange and evaporation from plants. Oak pollen, however, are relatively large (ca. 27 μm). Thus, their settling is mainly a function of sedimentation velocity. The deposition process is thus neglected. This simplification is based on the assumption that particles bigger than 10 μm are deposited independent of the roughness of the surface [50].

Sedimentation velocity of the pollen was assumed to be constant during a 1-day simulation. A list of previous and recent articles on sedimentation veloci-

ties of several pollen species is given by Jackson and Lyford [21]. For oak species, miscellaneous authors estimated the pollen sedimentation velocity in a range of 1.83–3.96 cm/s ([21] p. 71). If we calculate the sedimentation velocity via Stokes' law for spherical particles [5] by using the different available measures of the size and density of oak pollen grains [21, 32], the sedimentation velocity is between 1.89 and 2.98 cm/s. We choose 2.9 cm/s as standard sedimentation velocity in all simulations.

All simulations with METRAS are being performed with relative pollen quantities (RPQ). The absolute pollen quantities (APQ) are calculated from the model results of a single day by multiplying the simulated $RPQs$ with the fraction of viable pollen grains k and with the pollen production ratio [p_R in equation (3)] of the corresponding day:

$$APQ = RPQkp_R. \tag{6}$$

3. Model area

The study region is located in North Germany between Hamburg and Lübeck (figure 1a). This landscape is characterized by relatively flat terrain containing only slight differences in elevation of about 100 m (figure 1b). Fragmented forests, cultivated fields, and pastures well separated by hedges adorn the rural landscape (figure 1c). Main owners of the forests are the city of Lübeck and the Herzogtum Lauenburg County, with a small area privately owned. Land-use and orography data are taken from the ATKIS digital landscape model 'Basis-DLM' and the digital terrain model 'DGM200.' These models were provided by the Federal Agency for Cartography and Geodesy (Frankfurt-am-Main, Germany 2002). Within this landscape the Institute for Forest Genetics and Forest Tree Breeding maintains the intensive study plot (ISP) 'Behlendorf' [6, 7, 47], from which the annual pollen production was estimated (Section 2.2.). The fate of oak pollen emitted from this stand was investigated in simulations. The ISP belongs to the communal forests of the city of Lübeck. The age of the 228 oak trees is estimated to be 183 years, the average height is 33 m, and the average diameter at breast height is 71 cm [6]. The whole stand has a size of about 4.65 ha. Digital maps of the oak stand and data from Basis-DLM and DGM200 were combined to create a topography data set with a rough landscape for the simulations. This data set was embedded in the computational domain with a size of 210 × 205 × 10 km. The vertical resolution is 20 m at the ground, and increases above with a factor of 1.2 to a maximal grid size of 1,000 m. The model top lies at a height of about 10,000 m. The horizontal resolution is non-uniform with a grid size of 500 m within the core area of the investigated landscape (32 × 28 km), and an increasing grid size (factor 1.2) to 5,000 m (see schematic representation in figure 1a). Topography data outside the core area contain land-use and height data in a resolution of 5 km without specific information about oaks. Together, the computational domain consisted of 115 × 106 horizontal and 32 vertical grid cells.

3.1. Meteorological situation

Simulations were performed for a meteorological situation based on the weather of April 30 and May 2 in year 2000. On these days, the lowest (April 30) and the highest (May 2) pollen concentrations were recorded at the pollen station Lübeck in the flowering period of year 2000 (figure 2). Simulations were initialized with average atmospheric soundings from Bergen, Schleswig and Greifswald (DWD Offenbach, Germany) taken at midnight of May 2 and April 30, respectively. For both 1-day simulations, the large-scale meteorological situation was kept constant, while the typical diurnal changes in the meteorological variables caused by the diurnal cycle were included in the model simulations. Simulations were performed with the ISP as the only pollen source in the model area (figure 1).

On April 30, ground fog was observed in the morning; thereafter, a cloudy sky with a maximum temperature of 19° C, a relative humidity of 70%, and a wind of 2 m/s from southwest were observed. In May 2, a maximum temperature of about 22° C, a sunshine duration of 7 h, a relative humidity of 60%, and a wind with approximately 4 m/s from north to northeast were recorded in the region of Hamburg–Lübeck.

4. Model results

The obtained simulation results were analyzed for the number of emitted pollen, horizontal pollen concentrations within in the lowest vertical grid cells, vertical pollen concentrations in the atmosphere, and pollen-settling pattern.

4.1. Pollen emission

Pollen emission in the stand 'Behlendorf' is displayed in figure 3 as the number of emitted pollen of 1 m^2 oak forest/s for the simulated days. On April 30, emission started at 7:13 A.M. with low values of a few 10 pollen/s

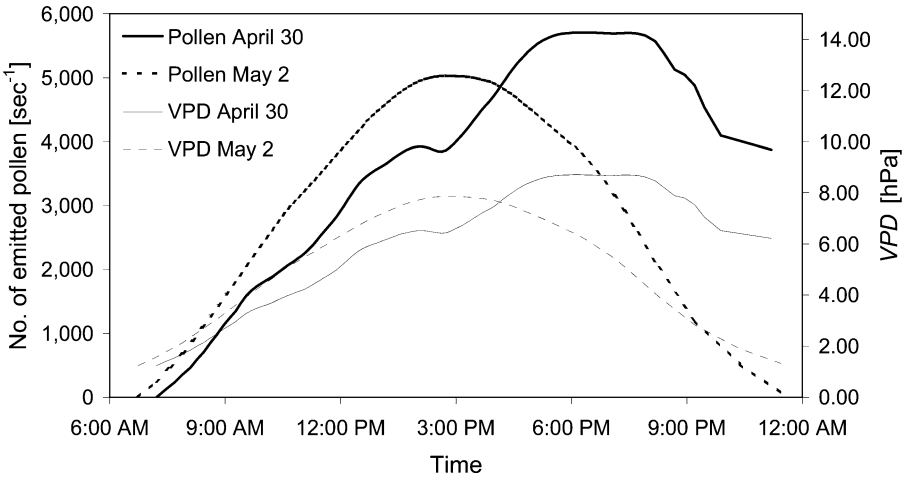

Figure 3 Pollen emission and vapor pressure deficit (VPD) for the 2 days simulated

and increased up to 5,700 pollen/s at 6:00 P.M. After 2 h with a continuous high emission, the emission decreased to 3,500 pollen/s at midnight. The total emission of 1 m^2 oak forest stand is 2×10^8 pollen on April 30. On May 2, emission started at 6:45 A.M. and constantly increased up to 5,030 pollen/s at 2:45 P.M. After 3:00 P.M. the emission decreased throughout the afternoon and evening, and reached zero emission around 11:40 A.M. The simulated emissions of 1 m^2 oak forest stand for May 2 amounted to 1.7-10^8 pollen in total.

Pollen emission includes all pollen, viable and dead pollen grains, as neither the initial pollen viability k nor pollen sensitivity to sunlight r_S affects the pollen emission. In contrast, the following descriptions of pollen concentration and pollen deposition belong only to the distribution of viable pollen.

4.2. Pollen concentration

The diurnal dynamics of pollen concentration in the lowest vertical layer (20 m) as horizontal and vertical cross-sections are given in figures 4 and 5 for the 2 days simulated. The horizontal cross-section displays 60 × 60 km of the simulated area, focused on the ISP as a single pollen source. The vertical cross-section cuts the ISP in south-north direction (40 km) and displays the concentration profiles up to a height of 1,500 m.

On April 30 (figure 4), moderate winds from south contributed to a relatively small pollen cloud of 20 km length around 6:30 P.M. Not surprisingly, the highest concentrations were found between 6:00 P.M. and 8:00 P.M. close to the source with more than 1,000 pollen/m^3. In the afternoon, the convection regime transports the pollen cloud with concentrations between 10 and 20 pollen/m^3 up to a height of 1,300 m. Vertical cross-sections for 6:30 P.M. and 8:30 P.M. show the horizontal transport towards north and the sinking of the pollen due to sedimentation as well as the stabilizing effect of the evening boundary layer.

On May 2 (figure 5), wind from northerly directions advects the pollen cloud to the south and southwest directions. The highest concentration values can be found directly at the pollen source with values between 300 and 1,000 pollen/m^3. The tip of the pollen cloud with concentrations between 3 and 10 pollen/m^3 extends up to 30 km. This longest stretch was found around 7:00 P.M., a few hours after the emission peak and with a wind speed of about 4m/s. The vertical cross-section illustrates the vertical transport of pollen that extends up to 600 m with concentrations between 10 and 20 pollen/m^3. The pollen cloud reached its highest altitude between 12:00 noon and 1:00 P.M.

4.3. Pollen deposition

The pollen deposition pattern of the simulated days is displayed in figure 6, showing the complete simulation area of 200 × 200 km (left) and a subsection of 60 × 60 km (right) that contains the ISP in its centre. Additionally, the area size on which a certain number of pollen deposited (encircled by the respective isolines) was calculated and is given in the legend. On April 30, a small number of 10-100 viable pollen/m^2 deposited in a region that spans 1,718 km^2. This area extends up to 70 km north of the pollen source. The area on which 1,000–10,000 pollen deposited per m^2 spans 156 km^2. A value of 1,000 pollen/m^2 can be seen as a critical value for pollination [45]. The largest pollen deposition occurred in an area of approximately 0.4 km^2 around the source, with more than 10^6 pollen/m^2. On May 2, 10–100 pollen/m^2 deposited on an area of 5,713 km^2, which extends to more than 100 km away from its source. However, sufficient pollen numbers for pollination (>1,000 pollen/m^2) were only

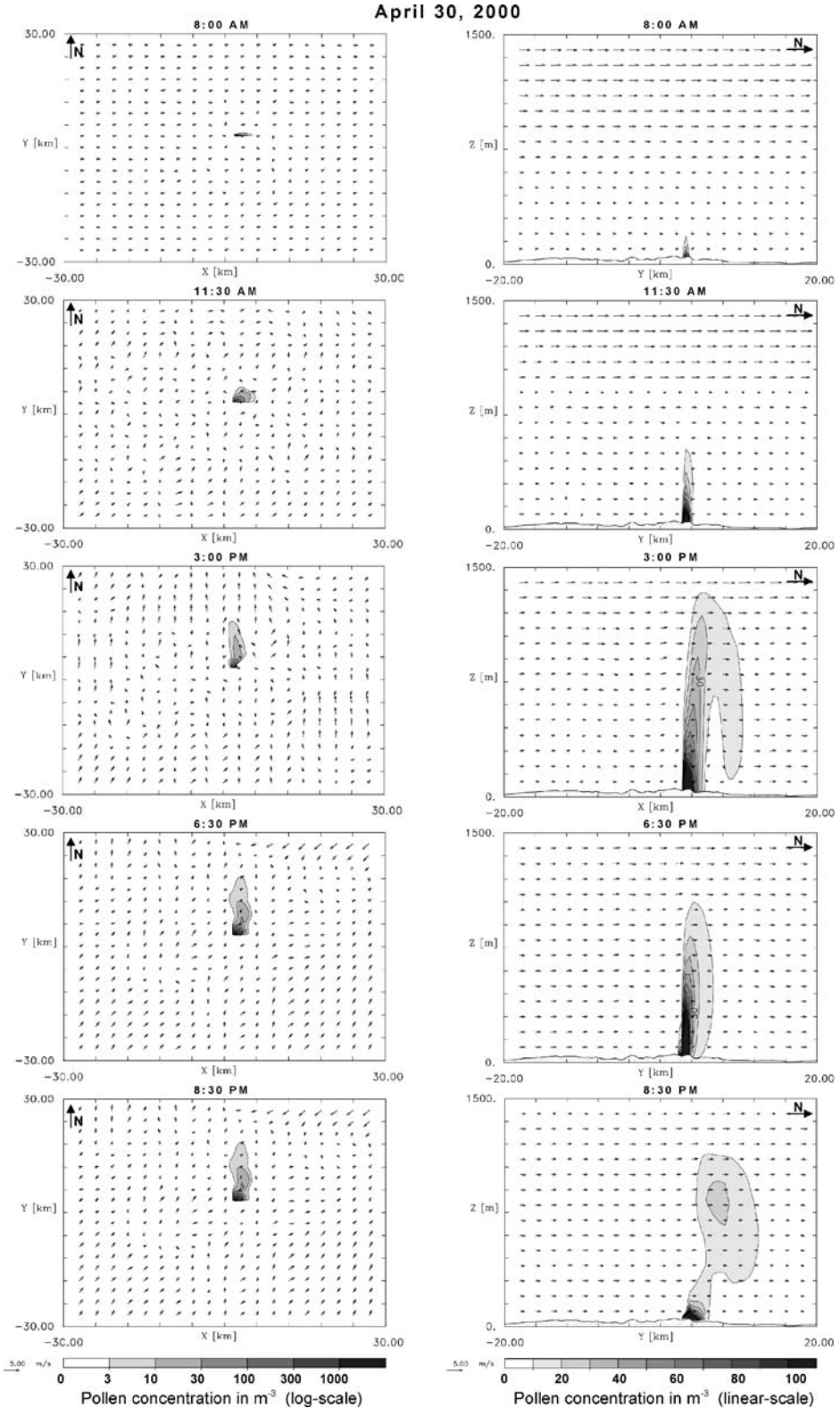

Figure 4 Diurnal spatial dynamics of the pollen concentration and the wind field within the atmosphere on April 30, 2000, at five selected times. The horizontal cross-section (left) depicts a 60×60 km sub-section of the simulation area in which the ISP as single pollen source was centered at the lowest vertical layer (20 m). The vertical cross-section (right) presents the height profiles up to 1,500 m on a 40-km transect in south–north direction through the ISP

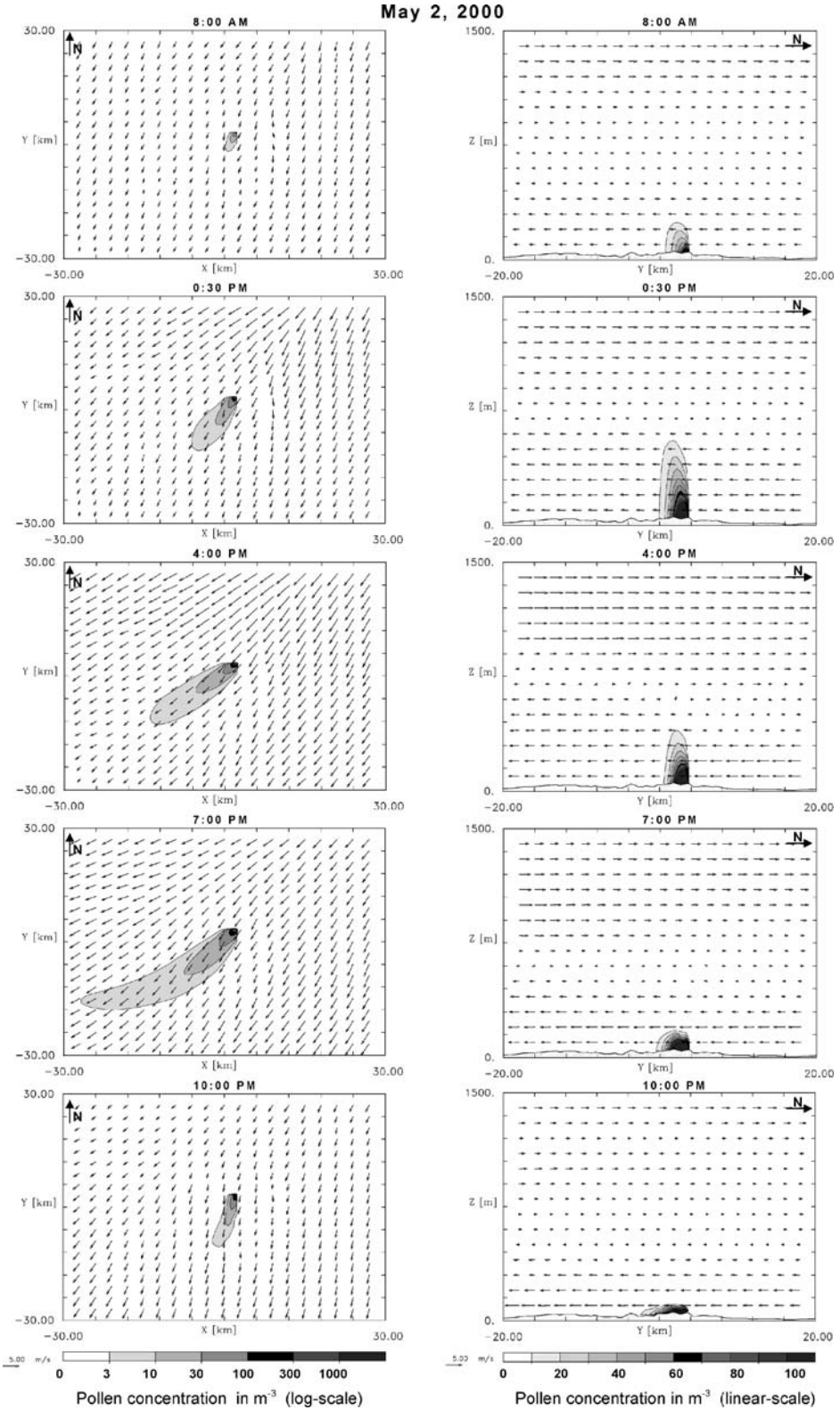

Figure 5 Same as figure 4, but for May 2, 2000

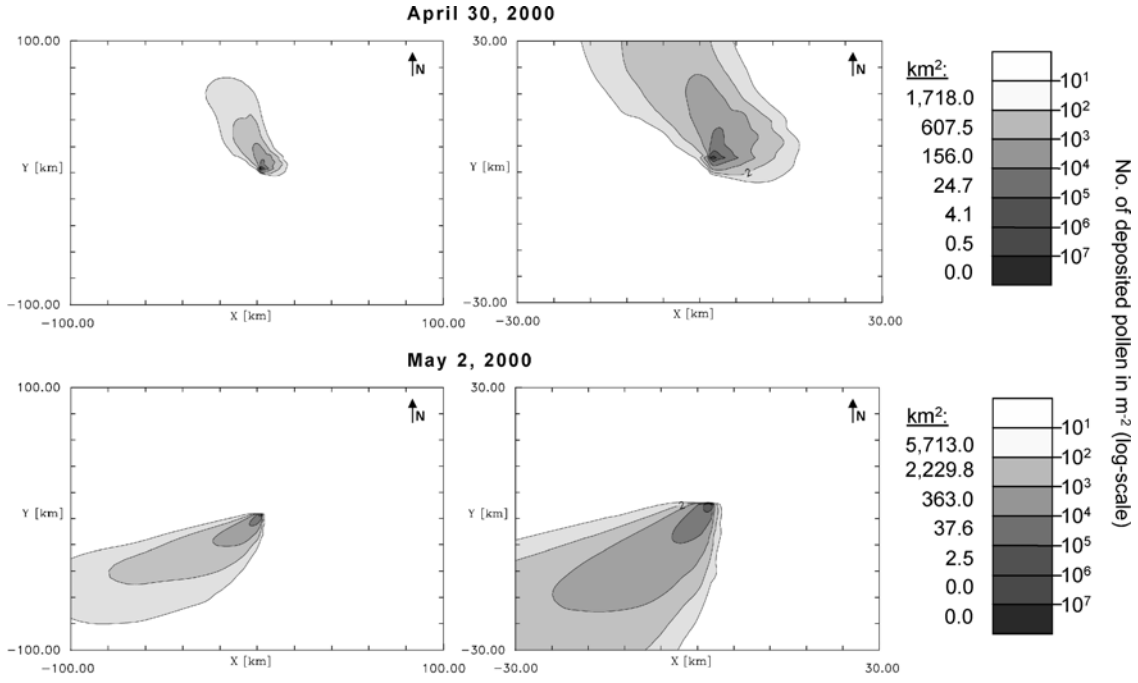

Figure 6 Pollen deposition pattern, integrated over 24 h. The horizontal cross-sections display the entire simulation area with 200 × 200km (left) and a more focused sub-section of 60 × 60 km (right). Beside the legend, the calculated area size with the specific number of pollen deposited is given. Top: April 30. Bottom: May 2

found in an area of 363 km^2, less than 25 km away from the source. The area with a very high number of deposited pollen (>10^5 pollen/m^2) has a size of 2.5 km^2.

5. Discussion

5.1. Usability of the approach for dispersal of pollen and gene flow

Mesoscale meteorological models are widely applied for the simulation of transport and chemical transformations of pollutants in the atmospheric boundary layer [40]. By considering pollen as particle in terms of atmospheric science, the state of atmospheric transport models can be taken as grant for their application to pollen dispersal. The quality of current transports models is within ± 50% of the measured concentration values, and mostly better for wind and other meteorological parameters [40, 42]. This is a good precondition for basing pollen dispersal models on meteorological transport models. In recent years, a few studies also evaluated the use of mesoscale models for pollen dispersion studies: the meteorological model MM5 was coupled with the Lagrangian dispersion model HYSPLIT_4 for predicting pollen concentrations of oak [33], the regional climate model RCM-NARCM was used to analyze a ragweed pollen cloud over a Canadian city [16], and the mesoscale model system KAMM/DRAIS was tested for Hazel and Alder pollen [18]. These studies were aimed at forecasting allergenic pollen concentrations in the atmosphere; and the parameterizations applied were derived from measurements [16] or from an assumed dependence of pollen release from the meteorological conditions [18, 33]. In contrast to these studies, the presented application of a mesoscale meteorological model is focused on pollen dispersal processes for a quantification of gene flow [45, 46] and the risk assessment of transgenic trees [9, 12]. This required the incorporation of biological relevant functions for pollen emission and pollen viability, and the parameterization of pollen production with empirical values. This combination of meteorological information from the mesoscale model system and biological parameters is a surplus when using meteorological models for investigating pollen dispersion. The biological functions affect the obtained dispersion and pollination pattern.

The most important of the biological variables is the parameterization of the pollen emission Q_{emi}, which was drawn from an experimental data set of 1937 [38]. The use of such an old data set was necessary since no newer simultaneous measurements of pollen concentration and meteorological conditions close to the source and with a high temporal resolution were available for deciduous trees. Despite the age of this data set, the derived parameterization result in a reasonable emission function if we compare the emission pattern

with other and newer, but more qualitative, descriptions of the pollen emission of oak. The pollen shedding of various white oak species were found to occur at days were relative humidity (*RH*) dropped below 45% and air temperature (*T*) reached 17-21°C [51]. These conditions occurred in the afternoon between 2 P.M. and 6 P.M. [51]. Also, the strongest pollen emission of a single oak tree was observed at a time when *RH* was lowest, between 2 P.M. and 3 P.M. [34]. This fits the results of our parameterization, which has its emission peak at 3 P.M. on May 2 and at 6 P.M. on April 30, the times with the highest *VDP*. *VPD* is strongly correlated with *RH* and air temperature (*T*). The use of *VPD*, instead of *RH* and *T*, enables the application of emission function for different spring flowering trees. While the parameters were derived for alder, which flowers in March, they produce convincing results for oak, which flowers in late April and May, and for poplar, which flowers in April (unpublished data). Nevertheless, an experimental determination of pollen emission and meteorological conditions in a high temporal resolution would be a step forward and required for detailed validations of the model.

Besides the diurnal dynamics of pollen emission due to changes in meteorological variables, the strength of emission depends on the availability of mature oak anthers. Following the idea of grass pollen forecasts [31], this relationship was modeled by a fourth-order polynomial function [equation (2)] that was adjusted to the regional pollen counts. This simplest solution to determine the pollen production of a specific day is rather descriptive and can only be applied after the flowering season is over. A use of this function for the flowering season of other years or to forecast the daily pollen release during flowering is inappropriate. To include such desirable features, detailed phenological observations of the flowering, pollen counts, and measurements of the meteorological conditions are necessary. A framework for the integration of these variables into pollen dispersal models, provided that sufficient data are available, is demonstrated by a model for the dispersion of airborne cedar pollen [22, 23].

The second biological parameter in the dispersion model is the total pollen production (P_T) within the flowering period. The present study describes one of the first attempts to estimate P_T. Relative pollen production ratios, which have been estimated for paleobotanical questions (e.g., [2, 35]), are not usable for a quantification of the source strength. A similar quantification of P_T was carried out by V. Jato and N. Dacosta (Department of Plant Biology and Soil Sciences, University of Vigo, Spain) for 2002 and 2003 in Spain. Their results (Jato, personal communication) and a comparison with the estimated values of this study suggest a high variability in the yearly pollen production by a factor of about 5, which should be accounted for within the model [45].

The third biological parameter, pollen viability Q_{viab}, was integrated into the model by taking into consideration the dependence of pollen viability on the level and length of solar irradiation that is characteristic for the flowering period of oak. A detailed description of this parameter and a sensitivity analysis is given elsewhere [48].

The METRAS model used here provides the opportunity to include more biological or chemical variables. For example, sedimentation velocity of the pollen that is assumed to be constant in the present study can be considered dependent on its moisture content and the atmospheric humidity [4], thereby considering the increasing weight of pollen by uptake of water vapor. This is very similar to atmospheric particle transport and similar approaches can be used [60].

5.2. Evaluation strategy and comparison of the simulated data with field studies

Experimental studies on pollen flow on the landscape level are difficult and rare. This is attributable to (i) the common and wide-ranging occurrence of wind-pollinated trees, (ii) difficulties in receiving representative measurements of pollen concentration and deposition in a temporal and spatial resolution comparable to the model, and (iii) uncertainty in assigning a collected pollen sample to a specific tree or forest stand. A quantitative evaluation of the model quality based on measured data is therefore not yet possible. However, we provide a qualitative evaluation where we compare simulation results with field data of pollen concentration and deposition studies. In our model, quality control consists of three steps: first, a comparison of the simulated weather situation with the observed meteorology; second, a comparison of the simulated pollen concentration pattern with available field data; and third, an analysis of the pollen deposition pattern with comparable data.

5.2.1. Comparison of meteorological data

Meteorological data from the simulations were compared with the actual meteorological conditions observed at the synoptic stations in the region (DWD Offenbach, Germany) according to the evaluation scheme of Schlünzen and Katzfey [42]. In addition,

bias (average difference of simulated and measured values) was calculated. On April 30, a good agreement is found for wind speed (hit rate 75%, bias -0.7 m/s), a satisfying result for dew point temperature (hit rate 51%, bias 1.1 K) and temperature (hit rate 40%, bias 2.8 K), and a weak result for wind direction (hit rate 20%, bias –46°). On May 2, a good agreement was again found for wind speed (hit rate 69%, bias –0.7 m/s) and temperature (hit rate 58%, bias 1.1 K), whereas dew point temperature (hit rate 33%, bias 2.5 K) and wind direction (hit rate 40%, bias –17°) achieved only moderate hit rates. Is should be noted that these differences can be partly explained by the large-scale meteorological situation that was kept constant during both of the 2 days.

Differences in the simulated and observed meteorological situation affect the pollen dispersion in the following manner: first, travel distance is quite reliable for both days, since wind speed is simulated well. Second, the differences in simulated wind directions affect the orientation of the pollen cloud within the landscape. This is not very relevant in the present investigations, since the size and shape of the pollen cloud should be quite similar in all directions. In addition, in the present study we are more interested in general results on pollen dispersion and not in a perfect hindcast of it. Third, for pollen emission water *VPD* [equation (4)] is important. *VPD* is not a measurement quantity, but has been calculated from measured and simulated values to estimate the reliability of pollen emission rates dependent on atmospheric humidity. The *VPD* values – which are, for April 30, mainly too high and, for May 2, mainly too low – will lead to an overestimation of pollen emission for April 30 and to an underestimation on May 2. Therefore, on May 2 higher pollen emission and consequentially a larger pollen cloud could be expected in reality, while on April 30 real pollen emissions were lower than simulated. The similarity in the simulated values for *VPD* can also explain the similarity of total pollen emission on the simulated days (April 30: 2×10^8 pollen, May 2: 1.7×10^8 pollen). Overall, accuracy of meteorological parameters is reasonable in the light of the applied stationary synoptic situation, and sufficient for the exemplary pollen dispersion simulations of this study.

5.2.2. Comparison of pollen concentration data

Simulated results for pollen concentrations fit well with the range of observed data on physical pollen dispersal. Empirical investigations revealed an oak pollen concentration of 700 pollen/m^3 measured with a Rotorod sampler and 3,000 pollen/m^3 measured with a Burkhard trap on the peak day of flowering within an oak stand [25]. In our simulations, the pollen concentration at the pollen source is between 1,000 and 10,000 pollen/m^3 on April 30, and between 100 and 1,000 pollen/m^3 on May 2. Considering the variability in the different sampling methods in the field, a sufficient agreement is given. Qualitative agreement is also found in the decrease in pollen concentration a few kilometers outside the oak stand, where a 'more than hundred times' lower concentration than inside the stand has been reported [25]. Also, in our simulations, the concentrations decrease to values smaller than 10 pollen/m^3 about 8 km downwind and a few hundred meters upwind of the stand.

The vertical concentration patterns can be compared with pollen sampling data from aircraft or balloon flights. On 15 flights over mountainous and flat terrain, significant amounts of up to 5 oak pollen/m^3 were found in heights ranging from 1,000 up to 3,000 m, depending on weather conditions and date of the flight [38]. Similar vertical pollen distribution patterns were observed during 29 flights over Long Island [37]. These flights measured oak pollen concentrations of up to 20 pollen/m^3 in heights up to 3,000 m [37]. Our simulations produce comparable vertical profiles with pollen distributed up to 1,300 m and distinct concentration peaks in higher altitudes (figure 4, 8:30 P.M.).

5.2.3. Comparison of pollen deposition data

Several studies have been conducted to determine the pollen deposition of species that are important paleobotanical indicators, one of which is oak. For example, the annual pollen deposition of oak was investigated at eight different sampling sites in Germany [17], but none of the traps was located close to an oak forest. In dependence of the location of the trap, pollen deposition values from 7×10^5 up to 1.4×10^7 pollen/m^2 (average values of 3 years) were found [17]. The pollen deposition of a complete flowering period within an oak stand and on various locations within the surrounding landscape was determined in a Danish woodland [57]. The highest numbers of deposited pollen within this study were found within the oak stand with approximately 2.7×10^7 pollen/m^2 sampled with roofed Tauber traps [56]. Other sampling stations 150-400 m away from the oak stand measured pollen depositions between 1×10^6 and 6×10^6 pollen/m^2. In our simulations, which represent – in contrast to these field studies – only 1 day within the flowering period, the number of deposited pollen extends to values $>10^6$ only within a very small area. A few

Table 2 Linear regression analysis on 2days of alder flowering (data from [38]) to determine the most important meteorological parameters that affect the pollen release.

	Day 1			Day 2		
	a	*b*	R^2	*a*	*b*	R^2
VPD [hPa]	33.07	−42.24	0.8712	31.36	−31.537	0.9882
RH [%]	−4.7111	334.11	0.8699	−2.3995	182.64	0.9587
ν[ms^{-1}]	71.817	10.111	0.9388	−9.2089	38.822	0.3329
T [°C]	19.512	33.39	0.8096	7.9187	33.122	0.324
VPD + ν	12.957	−13.817	0.9511	−3.0601	33.972	0.0142

hundred meters away from the pollen source, the pollen deposition decreases to values between 0 and much lower than 10^6, depending on the simulated meteorological situation. If we consider the different time scale, the uncertainty of the pollen traps, and the single oak stand considered for pollen emission in our present study, the simulated results and the results of the mentioned field studies are within the same range. A better agreement cannot be expected in regard of the many unknown parameters in such a comparison.

5.2.4. Towards a more validated model

Mesoscale meteorology and tracer transport models are widely applied. Together with accurate meteorological parameterizations, these models have already been validated. They provide a high level of accuracy for the meteorological situation and transport of physical tracers [40, 42], provided the initial and boundary values are sufficiently close to reality. Thus, mesoscale meteorological models can be used as meteorological drivers for pollen dispersion studies without further extensions.

In contrast, the biological parameterizations used in the model were derived from rough estimates and from some very rare experimental investigations. Thus, more experimental studies using up-to-date measurement equipment are essential to improve and validate the biological functions involved in pollen emission and viability.

A validation of the combined model including meteorology and pollen dispersal requires representative measures of pollen concentration and pollen deposition over a complete flowering period with a resolution of hours. Moreover, it requires selecting a specific landscape/tree species combination, where the simulated tree species should be restricted to a very few stands as pollen sources, while the landscape itself and the climate conditions should be typical for the selected species. Only within such a landscape can we expect a reliable assignment of pollen samples to a given pollen source. Validation should also include analysis of pollen viability from the pollen samples and should be combined with a genetic analysis of the sampled pollen or the seeds that emerged after the analyzed pollination period. Together, these data will help us to evaluate mesoscale pollen dispersal models for various purposes, e.g., gene flow, allergy monitoring, or atmospheric aerosol load, where pollen also play a role.

6. Conclusion

The present study describes the successful extension and application of a mesoscale meteorological model to simulate the emission and dispersion of windborne pollen. This approach enables the study of pollen dispersion and pollination on the landscape level by considering landscape structure, local meteorological conditions during flowering, and biological parameters of the pollen, e.g., diurnal cycle of pollen emission, total pollen production, pollen viability. Due to difficulties encountered in measuring pollen dispersal on a landscape level, a quantitative validation has not been carried out within the present study. A qualitative evaluation revealed that simulated values of pollen concentration and emission lay within the range of published field data.

The application of mesoscale meteorological models for pollen dispersal is a promising approach for the management of wind-pollinated trees in fragmented landscapes, and for risk assessment studies of transgenic trees. However, further studies would aid these applications. Besides a revision of the referred biological parameters with more experimental data, further extensions may include: (i) use of a higher-resolution model (less than 500 × 500 m) for a better representation of the landscape structure; (ii) use of nested simulations with dynamic boundary conditions for a higher accuracy of the meteorological conditions, which proved to be an important factor for pollen emission and dispersion; (iii) distinction between pollen from

different stands for a consideration of pollen competition; and (iv) study of pollen dispersion within a stand, where obstacle and vegetation resolving atmospheric models (e.g., [41]) might be adapted.

Acknowledgements We gratefully acknowledge the assistance of Alexandra Tusch and Dieter Boedecker (Institute for Forest Genetics and Forest Tree Breeding, Groβhansdorf, Germany) by estimating the pollen production of *Q. robur* at the ISP, and would like to thank Alfred Trukenmüller (Meteorological Institute, University of Hamburg) for help in the integration of the emission function into METRAS. Special thanks go to Victoria Jato Rodríguez and Nuria Dacosta Quiroga (Department of Plant Biology and Soil Sciences, University of Vigo, Spain) for kindly providing unpublished data of the pollen production of *Q. robur*. Thanks also go to the forest services of Farchau and Lübeck (Germany) for GIS-based maps of the forest inventory, to the German Pollen Foundation (Bad Lippspringe, Germany) for the pollen counts in Lübeck, to the Federal Agency for Cartography and Geodesy (Frankfurt a. Main, Germany) for digital land-use and topography maps and to the German Weather Service (Offenbach, Germany) for providing meteorological measurements for model evaluation. For many helpful discussions and hints we are grateful to Florian Scholz, who also initiated and supported this project together with Heike Hertel (Institute for Forest Genetics and Forest Tree Breeding, Groβhansdorf and Waldsieversdorf). This work is part of a joint project funded by the German Federal Ministry of Consumer Protection, Food, and Agriculture (BMVEL): "On biological diversity of forests in Germany."

1. Appendix

A. Regression analysis to identify the most important meteorological factors for pollen release

Regression analysis was made from measurements of pollen concentration within an alder crown and the synchronous record of relative humidity (RH), temperature (T), and wind speed ($|v|$). From temperature and relative humidity, we calculated the water vapor pressure deficit (VPD) according to the formulae

$$VPD = e_{sat} - e_{curr} \tag{A1}$$

with the saturation vapor pressure (e_{sat}, hPa) following MAGNUS:

$$e_{sat} = \begin{cases} 6.1078\, e^{\frac{22.44294 T_a}{272.44+T_a}} & \text{for temperature } T_a < 0^\circ C \\ 6.1078\, e^{\frac{17.08085 T_a}{234.175+T_a}} & \text{for temperature } T_a \geq 0^\circ C \end{cases} \tag{A2}$$

and the current water vapor pressure (e_{curr}, hPa):

$$e_{curr} = e_{sat} \frac{RH}{100}. \tag{A3}$$

Regression analysis was made with every meteorological factor (RH, T, $|v|$), with VPD, and with a combination of the water vapor pressure deficit and the wind speed ($VPD + |v|$). Table 2 shows the results of the linear regression ($f(x)=ax + b$) and the coefficient of determination (R^2) for the 2 days; data are available from [38].

B. Consideration of changes in pollen viability during transport in Eulerian models

Integration of equation (1) forward in time results in:

$$\begin{aligned} C^{i+1} = & C^i \\ & + \Delta t \Big(- \nabla \overline{C}\overline{v}|^i - \nabla \overline{C'v'}|^i + Q_{emi}|^i + Q_{sed}|^i \Big) \\ & - \Delta t Q_{viab}|^i, \end{aligned} \tag{B1}$$

where C^{i+1} describes the concentration at time step $i + 1$ and C^i indicates the concentration at time step i. When summarizing all terms, except Q_{viab}, on the right-hand side of (B1) to $\widehat{C}^{i+1}$, equation (B1) reads:

$$C^{i+1} = \widehat{C}^{i+1} - \Delta t Q_{viab}\big|^i. \tag{B2}$$

With the pollen survival rate V_S, given in equation (5), C^{i+1} results in:

$$C^{i+1} = \widehat{C}^{i+1} V_S. \tag{B3}$$

Rearranging gives the following relation for Q_{viab}:

$$Q_{viab} = \frac{(1 - V_S)}{\Delta t} \widehat{C}^{i+1}. \tag{B4}$$

References

1. Aas, K., Aberg, N., Bachert, C., Bergmann, R., Bonini, S., Bousquet, J., et al. (1997). *European allergy white paper: Allergic diseases as a public health problem*. Brussels: The UCB Institute of Allergy.
2. Andersen, S. T. (1970). The relative pollen productivity and pollen representation of north European trees, and correction factors for tree pollen spectra, Geological Survey of Denmark, II. Series, No. 96.
3. Austerlitz, F., & Garnier-Géré, P. H. (2003). Modelling the impact of colonisation on genetic diversity and differentiation of forest trees: Interaction of life cycle, pollen flow and seed long-distance dispersal. *Heredity*, *90*, 282 – 290.
4. Aylor, D. E. (2002). Settling speed of corn (*Zea mays*) pollen. *Journal of Aerosol Science*, *33*, 1601 – 1607.
5. Chamberlain, A. C. (1975). The movement of particles in plant communities. In J. L. Monteith (Ed.), *Vegetation and the atmosphere, Vol. 1* (pp. 155 – 203). London: Academic Press.

6. Degen, B., Llamas-Gomez, L., & Scholz, F. (1999). Erarbeitung von Entscheidungshilfen für eine nachhaltige Forstwirtschaft zum Schutze der genetischen Vielfalt von Waldbaum- und Waldstraucharten. In F. Scholz & B. Degen (Eds.), *Wichtige Einflussfaktoren auf die Biodiversität in Wäldern, BFH-Mitt. No. 195* (pp. 1 – 139). Hamburg: Max Wiedebusch.
7. Degen, B., Streiff, R., & Ziegenhagen, B. (1999). Comparative study of genetic variation and differentiation of two pedunculate oak (*Quercus robur*) stands using microsatellite and allozyme loci. *Heredity*, *83*, 597 – 603.
8. Dierer, S., Schlünzen, K. H., Birnbaum, G., Brümmer, B., & Müller, G. (2005). Atmosphere-sea ice interactions during a cyclone passage investigated by using model simulations and measurements. *Monthly Weather Review*, *133*, 3678 – 3692.
9. DiFazio, S. P., Slavov, G. T., Burczyk, J., Leonardi, S., & Strauss, S. H. (2004). Gene flow from tree plantations and implications for transgenic risk assessment. In C. Walter & M. Carson (Eds.), *Plantation forest biotechnology for the 21st century* (pp. 405 – 422). Kerala: Research Signpost 37/661.
10. Dow, B. D., & Ashley, M. V. (1998). High levels of gene flow in bur oak revealed by paternity analysis using microsatellites. *Journal of Heredity*, *89*, 62 – 70.
11. Ellstrand, N. C. (1992). Gene flow by pollen: Implication for the plant conservation genetics. *Oikos*, *63*, 77 – 89.
12. Fladung, M. (2004). Modellierung des Genflusses für die Risikoabschätzung gentechnisch veränderter Bäume. Working Paper No. 2004/4, Institute for Forest Genetics and Forest Tree Breeding, Federal Research Centre for Forestry and Forest Products, Hamburg.
13. Gerber, S., Mariette, S., Streiff, R., Bodénès, C., & Kremer, A. (2000). Comparison of microsatellites and amplified fragment length polymorphism markers for parentage analysis. *Molecular Ecology*, *9*, 1037 – 1048.
14. Giddings, G. (2000). Modelling the spread of pollen from *Lolium perenne*. The implications for the release of wind-pollinated transgenics. *Theoretical and Applied Genetics*, *100*, 971 – 974.
15. Giddings, G. D., Sackville Hamilton, N. R., & Hayward, M. D. (1997). The release of genetically modified grasses. Part 2: The influence of wind direction on pollen dispersal. *Theoretical and Applied Genetics*, *94*, 1007 – 1014.
16. Goyette-Pernot, J., Muñoz-Alpizar, R., Blanchet, J.-P., Goyette S., & Beniston, M. (2003). Analysing ragweed pollen cloud over Montreal City Center, in: Proceedings of the 5th International Conference on Urban Climate, Lodz.
17. Grosse-Brauckmann, G. (1978). Absolute Pollenniederschlagsmengen an verschiedenen Beobachtungsorten in der BRD. *Flora*, *167*, 209 – 247.
18. Helbig, N., Vogel, B., Vogel, H., & Fiedler, F. (2004). Numerical modelling of pollen dispersion on the regional scale. *Aerobiologia*, *20*, 3 – 19.
19. Hidalgo, P. J., Mangin, A., Galán, C., Hembise, O., Vázquez, L. M., & Sanchez, O. (2002). An automated system for surveying and forecasting Olea pollen dispersion. *Aerobiologia*, *18*, 23 – 31.
20. Hirst, J. M. (1952). An automatic volumetric spore trap. *Annals of Applied Biology*, *39*, 257 – 265.
21. Jackson, S. T., & Lyford, M. E. (1999). Pollen dispersal models in Quaternary plant ecology: Assumptions, parameters, and prescriptions. *Botanical Review*, *65*, 39 – 75.
22. Kawashima, S., & Takahashi, Y. (1995). Modelling and simulation of mesoscale dispersion process for airborne cedar pollen. *Grana*, *34*, 142 – 150.
23. Kawashima, S., & Takahashi, Y. (1999). An improved simulation of mesoscale dispersion of airborne cedar pollen using a flowering-time map. *Grana*, *38*, 316 – 324.
24. Klein, E. K., Lavigne, C., Foueillassar, X., Gouyon, P. H., & Laredo, C. (2003). Corn pollen dispersal: Quasi-mechanistic models and field experiments. *Ecological Monographs*, *73*, 131 – 150.
25. Lahtinen, M.-L., Pulkkinen, P., & Helander, M. L. (1997). Potential gene flow by pollen between English oak (*Quercus robur* L.) stands in Finland. *Forestry Studies*, *28*, 47 – 50.
26. Levin, D. A, & Kerster, K. W. (1974). Gene flow in seed plants. *Evolutionary Biology*, *7*, 139 – 220.
27. Loos, C., Seppelt, R., Meier-Bethke, S., Schiemann, J., & Richter, O. (2003). Spatially explicit modelling of transgenic maize pollen dispersal and cross-pollination. *Journal of Theoretical Biology*, *225*, 241 – 255.
28. Loveless, M. D., & Hamrick, J. L. (1984). Ecological determinants of genetic-structure in plant-populations. *Annual Review of Ecology and Systematics*, *15*, 65 – 95.
29. Lüpkes, C., & Schlünzen, K. H. (1996). Modelling the Arctic convective boundary-layer with different turbulence parameterizations. *Boundary-Layer Meteorology*, *79*, 107 – 130.
30. Niemeier, U., & Schlünzen, K. H. (1993). Modelling steep terrain influences on flow patterns at the Isle of Helgoland. *Beiträge zur Physik der Atmosphäre*, *66*, 45 – 62.
31. Norris-Hill, J. (1995). The modelling of daily poaceae concentrations. *Grana*, *34*, 182 – 188.
32. Olsson, U. (1975). On the size and microstrucure of pollen grains of *Quercus robur* and *Quercus petraea* (Fagaceae). *Botaniska Notiser*, *128*, 256–264.
33. Pietrowicz, J., & Pasken, R. (2002). Testing of mesoscale meteorological models as a tool to forecast pollen concentrations, Workshop paper, 12th PSU/NCAR Mesoscale Modelling System Users' Workshop NCAR.
34. Pohl, F. (1933). Freilandversuche zur Bestäubungsökologie der Stieleiche. *Beihefte zum Botanischen Centralblatt*, *51*, 673 – 692.
35. Pohl, F. (1936). Die Pollenerzeugung der Windblütler. *Beihefte zum Botanischen Centralblatt*, *56*, 365 – 470.
36. Rajora, O. P., & Mosseler, A. (2001). Challenges and opportunities for conservation of forest genetic resources. *Euphytica*, *118*, 197 – 212.
37. Raynor, G. S., Hayes, J. V., & Ogend, E. C. (1974). Mesoscale transport and dispersion of airborne pollens. *Journal of Applied Meteorology*, *13*, 87 – 95.
38. Rempe, H. (1937). Untersuchungen über die Verbreitung des Blütenstaubes durch die Luftströ\mungen. *Planta*, *27*, 93 – 147.
39. Schlünzen, K. H. (1990). Numerical studies on the inland penetration of sea breeze fronts at a coastline with tidally flooded mudflats. *Beiträge zur Physik der Atmosphäre*, *63*, 243 – 256.
40. Schlünzen, K. H. (2002). Simulation of transport and chemical transformations in the atmospheric boundary layer — review on the past 20years developments in science and practice. *Meteorologische Zeitschrift*, *11*, 303 – 313.
41. Schlünzen, K. H., Hinneburg, D., Knoth, O., Lambrecht, M., Leitl, B., López, S. et al. (2003). Flow and transport in the obstacle layer: First results of the micro-scale model MITRAS. *Journal of Atmospheric Chemistry*, *44*, 113 – 130.
42. Schlünzen, K. H., & Katzfey, J. J. (2003). Relevance of sub-grid-scale land-use effects for mesoscale models. *Tellus*, *55A*, 232 – 246.

43. Schlünzen, K. H., & Pahl, S. (1992). Modification of dry deposition in a developing sea-breeze circulation — a numerical case study. *Atmospheric Environment*, *26*, 51 – 61.
44. Schlünzen, K. H., Stahlschmidt, T., Rebers, A., Niemeier, U., Kriews, M., & Dannecker, W. (1997). Atmospheric input of lead into the German Bight — a high resolution measurement and model case study. *Marine Ecology-Program Series*, *156*, 299 – 309.
45. Schueler, S. (2005). Pollen-mediated gene flow of trees in the temperate zone. PhD thesis, Department of Biology, University of Hamburg, Sierke Verlag, Göttingen.
46. Schueler, S., Degen, B., & Scholz, F. (2003). Muster genetischer Diversität in Waldbaumpopulationen-Wirkungen von Forstwirtschaft und Fragmentierung. *Nova Acta Leopoldina NF*, *87/328*, 395 – 399.
47. Schueler, S., Scholz, F., & Liesebach, H. (2004). Die Bedeutung des Genflusses für die Erhaltung der genetischen Vielfalt von Populationen in fragmentierten Landschaften, Working Paper No. 2004/2, Institute for Forest Genetics and Forest Tree Breeding, Federal Research Centre for Forestry and Forest Products, Hamburg.
48. Schueler, S., Schlünzen, K. H., & Scholz, F. (2005). Viability and sunlight sensitivity of oak pollen and its implications for pollen-mediated gene flow. *Trees*, *19*, 154 – 161.
49. Schulz, M., van Beusekom, K., Brockmann, U., Dannecker, W., Gerwig, H., Grassl, H., et al. (1999). The atmospheric impact on fluxes of nitrogen, POPs and energy in the German Bight. *Deutsche Hydrographische Zeitschrift*, *51*, 133 – 154.
50. Sehmel, G. A. (1980). Particel and gas dry deposition: A review. *Atmospheric Environment*, *14*, 983 – 1011.
51. Sharp, W. M., & Chrisman, H. H. (1961). Flowering and fruiting in the white oaks. I. Staminate flowering through pollen dispersal. *Ecology*, *42*, 365 – 372.
52. Sheng, L., Schlünzen, K. H., & Wu, Z. (2000). Three-dimensional numerical simulation of the mesoscale wind structure over Shandong peninsula. *Acta Meteorologia Sinica*, *1*, 97 – 107.
53. Siljamo, P., Sofiev, M., & Ranta, H. (2004). An approach to simulation of long-range atmospheric transport of natural allergens: An example of birch pollen. In Pre-prints of 27th Int. Technical Meeting on Air Pollution Modelling and its Applications, Banff, (pp. 395 – 402).
54. Smouse, P. E., Dyer, R. J., Westfall, R. D., & Sork, V. L. (2001). Two-generation analysis of pollen flow across a landscape. I. Male gamete heterogeneity among females. *Evolution*, *55*, 260 – 271.
55. Streiff, R., Ducousso, A., Lexer, C., Steinkellner, H., Gloessl, J., & Kremer, A. (1999). Pollen dispersal inferred from paternity analysis in a mixed oak stand of *Quercus robur* L. and *Q. petraea* (Matt.) Liebl. *Molecular Ecology*, *8*, 831 – 841.
56. Tauber, H. (1974). A static non-overload pollen collector. *New Phytologist*, *73*, 359 – 369.
57. Tauber, H. (1977). Investigations of aerial pollen transportation in forested area. *Dansk Botanisk Arkiv*, *32*, 1 – 121.
58. Thunis, P., Galmarini, S., Martilli, A., Clappier, A., Andronopoulos, S., Bartzis, J., et al. (2003). An intercomparison exercise of mesoscale flow models applied to an ideal case simulation. *Atmospheric Environment*, *37*, 363 – 382.
59. von Salzen, K., Claussen, M., & Schlünzen, K. H. (1996). Application of the concept of blending height to the calculation of surface fluxes in a mesoscale model. *Meteorologische Zeitschrift NF*, *5*, 60 – 66.
60. von Salzen, K., & Schlünzen, K. H. (1999). Simulation of the dynamics and composition of secondary and marine inorganic aerosols in the coastal atmosphere. *Journal of Geophysical Research-Atmosphere*, *23*, 30201 – 30217.
61. Winkler, H., Ostrowski, R., & Wilhelm, M. (2001). *Pollenbestimmungsbuch der Stiftung Deutscher Polleninformationsdienst*. Paderborn: Takt-Verlag.